

Recyclable Pd-contained perovskite catalyst synthesized by a low temperature hydrothermal method for aerobic alcohol oxidation



Leo Saputra^{a,b}, Takashi Kojima^a, Takayoshi Hara^a, Nobuyuki Ichikuni^a, Shogo Shimazu^{a,*}

^a Department of Applied Chemistry and Biotechnology, Graduate School of Science and Engineering, Chiba University, 1-33 Yayoi, Inage, Chiba, 263-8522, Japan

^b Department of Chemistry, Faculty of Mathematics and Natural Sciences, Riau University, Pekanbaru, 28293, Indonesia

ARTICLE INFO

Keywords:

Pd-contained perovskite
Intelligent catalyst
Hydrothermal synthesis
Aerobic alcohol oxidation

ABSTRACT

We successfully prepared Pd-containing perovskite strontium titanate (Pd-STO) by a relatively low-temperature hydrothermal method (*i.e.*, 373 K) without posterior calcination. The particle size and porosity of the STO perovskite could be tuned by changing the molar ratio of H₂O/NH₃ (*e.g.*, 5.0, 12.5 and 25.0) during the preparation of the amorphous titania sources. The mesoporous contained Pd-STO(12.5) showed superior catalytic performance compared to that of the other Pd-STO(*x*) (*x* = H₂O/NH₃) perovskites for alcohol oxidation with molecular oxygen. Both the refluxing of the non-polar solvents and addition of molecular sieves enhanced the reaction yield significantly. The Pd-incorporated perovskite (Pd-STO) showed better recyclability compared with that of the impregnated perovskite (*imp*-Pd/STO).

1. Introduction

The role of supports (*e.g.*, carbon, silica and alumina) in heterogeneous transition-metal catalysis is frequently crucial. The choice of an appropriate support can enhance the performance of transition-metal catalysts [1]. However, the recovery of the supported metal catalyst, especially platinum group metals (pgms), is still a major problem due to leaching or sintering [2,3]. This issue can be addressed using a pgm-contained perovskite catalyst [1].

Perovskite ABO₃ oxides (A = rare/alkaline earth, B = transition metals) are low-cost materials with high thermal stability and controllable physicochemical properties [4]. Appropriate changes in the perovskite composition (*i.e.*, partial substitution at B-sites with pgms) can lead to various and interesting magnetic, (thermo)electric, piezoelectric and catalytic properties [5]. The incorporation of a pgm into the perovskite lattice can also enhance its reusability. For example, Pd on perovskite could be reversibly reincorporated into the lattice, which is referred to as an “intelligent catalyst” [6], thus maintaining high dispersion and preventing leaching or aggregation, instead of on conventional supports (Fig. 1).

Pd-contained perovskite is usually prepared by conventional solid-state [7], co-precipitation [8] and sol-gel (Pechini) [9] methods. However, posterior calcination at a very high temperature (≥ 873 K) is required in these conventional methods. In a previous report, we used a molten-salt method (873 K) for Pd-contained perovskite fabrication (*i.e.*, Pd-STO, STO = SrTiO₃). The surface area of the resulting Pd-STO

was very low ($S_{\text{BET}} \leq 11 \text{ m}^2 \text{ g}^{-1}$), as commonly observed for perovskite, and almost inactive for low-temperature alcohol oxidation (353 K, yield: 12%) [10].

Unlike the abovementioned conventional methods, a hydrothermal method has been rarely studied for Pd-contained perovskite fabrication [11]. The significant advantages of this method are the controlled size and morphology, low-temperature growth and no posterior calcination [12]. In the present work, we successfully synthesized a Pd-STO perovskite with tunable particle size and porosity by using a low-temperature hydrothermal method (373 K) without any posterior calcination. The mesoporous-contained Pd-STO(12.5) showed the highest catalytic activity for aerobic alcohol oxidation among the Pd-STO(*x*) (*x* = H₂O/NH₃) materials. We showed that a refluxing of the non-polar solvents (*n*-hexane, *n*-heptane and cyclohexane) and addition of molecular sieves were required for obtaining the high yield (> 99%). The incorporation of Pd into the perovskite enhanced its recyclability compared with that of the impregnated perovskite.

2. Experimental

2.1. Chemicals

PdCl₂·2NaCl·3H₂O (95%), aqueous NH₃ (28%), 1-butanol (BuOH) (99%), acetonitrile (MeCN) (99.5%), Sr(OH)₂·8H₂O (90%), ethanol (99.5%), KOH (85%), benzyl alcohol (99%), 1-phenylethanol (98%), benzoin (98%), 1-octanol (98%), α -cyclopropylbenzyl alcohol (99%), *n*-

* Corresponding author.

E-mail address: shimazu@faculty.chiba-u.jp (S. Shimazu).

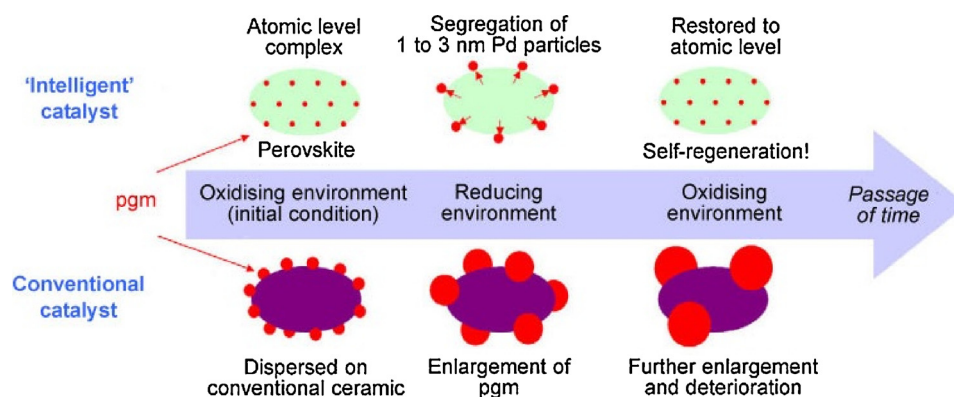


Fig. 1. Self-regenerative Pd-contained perovskite as an “intelligent catalyst” [1,3].

decane (99%), HNO_3 (60%) and molecular sieve (MS3A) pellets 3A 1/16 (pre-activated at 593 K for 6 h) were purchased from WAKO Chemicals. Crotyl alcohol (> 95%), 2-adamantanol (> 98%), *trans*-2-hexenol (> 95%), cyclooctanol (> 98%), 4-*tert*-butylcyclohexanol (98%), and 2-octanol (98%) were purchased from TCI Chemicals. $\text{Ti}(\text{O}i\text{Bu})_4$ monomer (99%) was purchased from Kishida Chameleon Reagent. All solvents (WAKO: *n*-hexane (96%), cyclohexane (98%), *n*-heptane (97%), toluene (99.5%), DMF (99.5%), 2-propanol (99.7%), 1,4-dioxane (99.5%), TCI: trifluorotoluene) were distilled prior to use. 1-Cyclohexylethanol (97%) and HCl (35%, for trace analysis grade) were purchased from Sigma Aldrich. Standard solutions (1000 ppm) of Pd, K, Sr, and Ti were purchased from WAKO Chemicals.

2.2. Preparation of the Pd-STO perovskite

The amorphous titania spheres (ATSS) were prepared by the direct hydrolysis of $\text{Ti}(\text{O}i\text{Bu})_4$, as described in our previous reports [13]. Briefly, 1.7 g (5 mmol) of $\text{Ti}(\text{O}i\text{Bu})_4$ was dissolved in BuOH/MeCN (1:1 v/v) (Solution A). A quantity of aqueous NH_3 and distilled water were also dissolved in BuOH/MeCN (1:1 v/v) (Solution B). The molar ratio of $\text{H}_2\text{O}/\text{NH}_3$ was varied at 5.0, 12.5 and 25.0. The ATSS are denoted as $\text{ATS}(x)$ with $x = \text{H}_2\text{O}/\text{NH}_3$. The two solutions were preheated at 353 K for 10 min, then mixed all together and stirred for 30 min. A white suspension was immediately formed and precipitated. The white precipitate was rinsed with ethanol and water and then dried at 348 K overnight.

Typically, the ATSS (2 mmol), $\text{Sr}(\text{OH})_2 \cdot 8\text{H}_2\text{O}$ (2 mmol), and Pd solution (0.028 mmol) were poured into a Teflon-lined autoclave (150 mL). Then, 20 mL of KOH 0.1 M and 80 mL of distilled water were also poured into the autoclave. Depending on the ATS sources, the perovskites were denoted as Pd-STO(x), with $x = \text{H}_2\text{O}/\text{NH}_3$. The mixture was homogenized under ultrasonic irradiation for 10 min. The autoclave was placed into an oven for a hydrothermal reaction at 373 K for 24 h. The obtained brown powder was rinsed with HNO_3 0.05 M and water, then dried at 348 K overnight. The chemical composition of the Pd-STO(12.5) based on ICP-OES analysis was $\text{Pd}_{1.0}\text{K}_{0.5}\text{Sr}_{78.5}\text{Ti}_{85.6}$ (Pd: 0.64 wt%). For comparison, a wetness impregnated catalyst (*imp*-Pd/STO) was also prepared with equal Pd loading.

2.3. Catalyst characterization

The Pd-STO catalysts were characterized by a powder XRD MiniFlex Rigaku instrument (Cu $K\alpha$, $\lambda = 1.5444$ nm) with a Ni $K\beta$ filter. The XRD instrument operated at 40 kV and 15 mA with a scan rate of 10°min^{-1} and a scan step of 0.1° . SEM images were obtained using an SEM JEOL JSM 6330F. N_2 adsorption-desorption isotherms were obtained at 77 K using a BELSORPmax instrument (BEL Japan). The samples were degassed at 423 K for 2 h prior to the measurement. TEM images were obtained using a Hitachi High-Tech H-7650 with an emissive gun, operated at 150 kV. Thermogravimetric (TG) analyses were performed on

a Rigaku Thermo plus Evo TG 8120 under a N_2 flow (250 mL min^{-1}) using Pt pans in the range of room temperature to 773 K (10 K min^{-1}). ICP-OES measurements were performed using a Thermo Scientific iCAP 7000 Series equipped with an Autosampler ASX-260 CETAC (Pd: 340.4589 nm, K: 766.4904 nm, Sr: 407.7718 nm, Ti: 334.9411 nm). The samples were dissolved in HCl 0.1 M prior to analysis.

2.4. Catalytic test

Pd-STO (12.5 mg), 1-phenylethanol (25 mg, 0.204 mmol), *n*-decane as an internal standard and *n*-hexane (2 mL) as the solvent were placed in a Schlenk flask equipped with reflux condenser, mechanical stirrer and balloon. The reaction was carried out at approximately the reflux temperature of *n*-hexane (342 K) under an O_2 atmosphere (0.1 MPa) for 24 h. In some cases, molecular sieves 3A (MS3A) were placed into the reaction mixture.

3. Results and discussion

3.1. Characterization of the Pd-STO catalysts

All of the ATS have monodispersed spherical shapes, as shown in the TEM (Fig. 2, a-c) and SEM (Fig. S3, a-c) images. Note that no precipitates were obtained in the absence of NH_3 and/or H_2O . The average particle sizes of $\text{ATS}(5.0)$ and $\text{ATS}(25.0)$ were approximately 0.5 μm , whereas the particle size of $\text{ATS}(12.5)$ was approximately 1.5 μm . All of the ATS contained microporous structures, as shown in the N_2 isotherm plot (Fig. S2). Although the particle size of $\text{ATS}(12.5)$ was relatively larger than the others, the specific surface area (S_{BET}) was significantly higher (Table S1) due to the presence of meso- and/or macroporous (Fig. 2b, Fig. S3 b). These ATSS were then used for the preparation of the Pd-contained perovskite.

After the hydrothermal reaction at 373 K, the particle size and shape of the Pd-STO corresponded to the ATS sources (Fig. 2d-f). In addition to the ATS sources, Pd-STO(12.5) also has the highest S_{BET} ($17.3 \text{ m}^2 \text{ g}^{-1}$). This value was quite higher than the value resulting from the molten-salt method ($\leq 11 \text{ m}^2 \text{ g}^{-1}$) [10]. Therefore, the $\text{H}_2\text{O}/\text{NH}_3$ ratio during ATS preparation is crucial for tuning the particle size and porosity of the resulting Pd-STO perovskites. All of the ATS sources could be used for perovskite formation, as shown in Fig. 3 c-e. The perovskite phase was confirmed and indexed to SrTiO_3 (JCPDS card 35–734). The Pd-STO perovskite could be obtained after a hydrothermal reaction at 373 K (Fig. S4). To the best of our knowledge, this is the lowest hydrothermal temperature for Pd-contained perovskite fabrication with tunable particle size and porosity. There were no other phases observed, confirming the high purity of the resulting perovskites. Additionally, we also used commercial TiO_2 anatase and rutile (not shown), but the perovskite phase was not formed, which proves the necessity of an amorphous titania source.

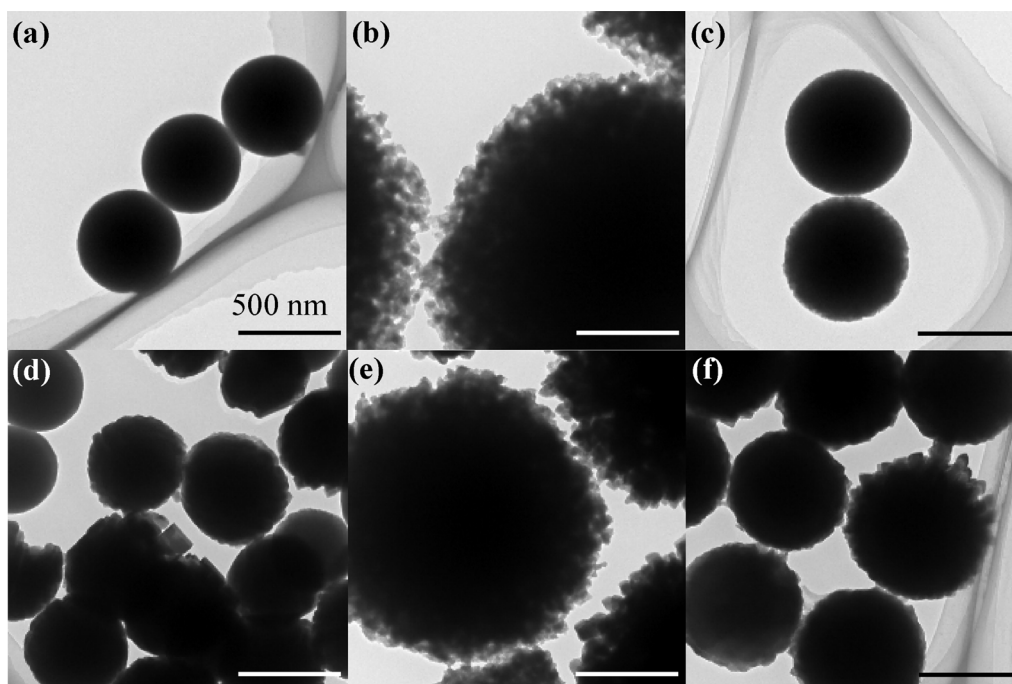


Fig. 2. TEM images of (a) ATS(5.0), (b) ATS(12.5), (c) ATS(25.0), (d) Pd-STO(5.0), (e) Pd-STO(12.5) and (f) Pd-STO(25.0). Scale bar = 500 nm.

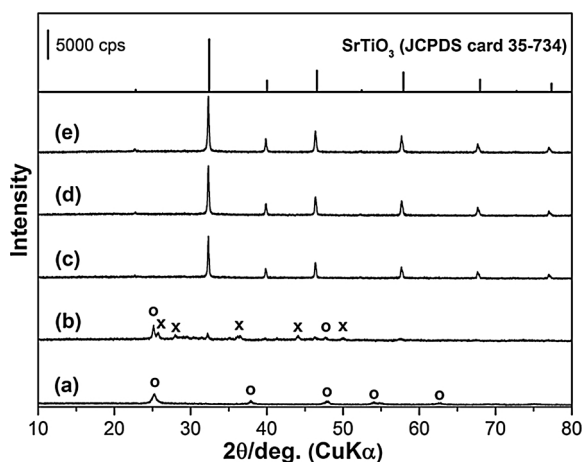


Fig. 3. Powder XRD patterns of (a) KTO(12.5), (b) Pd-STO(12.5) prepared by reflux method (373 K), (c) Pd-STO(5.0), (d) Pd-STO(12.5) and (e) Pd-STO(25.0). X = SrCO₃, O = TiO₂ (anatase).

The necessity of pressure during the hydrothermal process was confirmed, while the perovskite phase was not completely formed by the reflux method at 373 K (Fig. 3b). Additionally, only TiO₂ anatase was obtained in the absence of the Sr source (Fig. 3a). No appreciable shift in the perovskite reflections was observed by a small addition of Pd, but the crystallinity was slightly decreased (Fig. S5). We could not find any peak of PdO or Pd⁰ due to the low Pd feeding amount, very small crystallite size, or overlapping of its 2θ position with the perovskite (PdO 34° and Pd 40°) [14]. Even with a 10-fold increase in Pd, the XRD patterns remained unchanged (Fig. S5). However, a small peak of PdO appeared after calcination at 923 K for 6 h (but not for lower Pd loaded samples).

Based on the ICP-OES analysis (Table S2), the amount of Pd in the Pd-STO(12.5) was 0.06 mmol g⁻¹ (0.64 wt%). This value is quite low for detection using XRD or TEM. The ratio of Sr/Ti was approximately 1, which agrees with the ABO₃ perovskite formula. The Pd-impregnated perovskite (*imp*-Pd/STO) showed an identical XRD pattern to the incorporated one. In TEM images with higher magnification (Fig. 4a), the PdO or Pd⁰ particles could also not be seen due to the very well-dispersed particles or the incorporation of Pd into the perovskite. However, the PdO particles (2–5 nm) were clearly seen on the *imp*-Pd/STO (Fig. 4b).

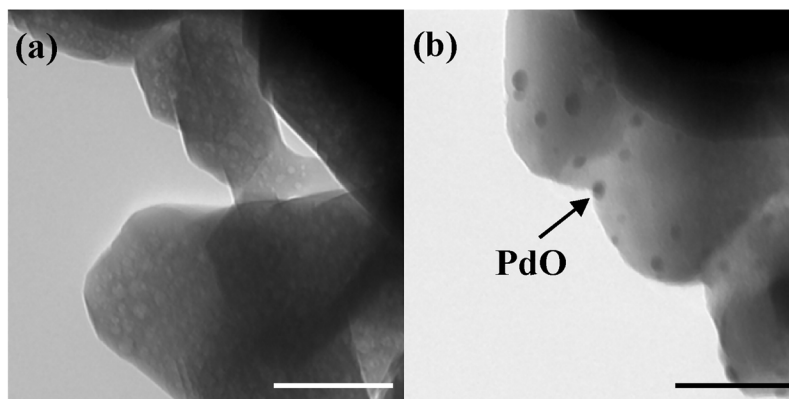
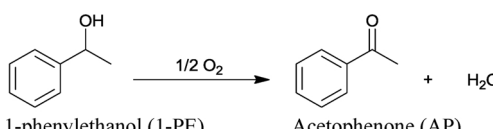


Fig. 4. TEM images of (a) Pd-STO(12.5) and (b) *imp*-Pd/STO(12.5). Pd loading: 0.64 wt%. Scale bar = 50 nm.

Table 1
Catalyst screening for the Pd-STO perovskites.



Entry	Pd-STO(x) ^a	Conv./%	Yield/% ^b	TON
1	Pd-STO(5.0)	31	31	85
2	Pd-STO(12.5)	63	63	172
3	Pd-STO(25.0)	54	54	147
4 ^c	Pd-STO(12.5)	36	36	98
5	STO(12.5)	0	0	0

Reaction conditions: 1-PE/Pd = 273; 1-PE, 25 mg; Pd-STO(x), 12.5 mg; *n*-hexane, 2 mL; O₂, 0.1 MPa (balloon); 342 K; 24 h.

^a x = [H₂O]/[NH₃].

^b The selectivity to AP is almost 100%. ^c The Pd-STO(12.5) was prepared at 433 K (hydrothermal).

3.2. Catalytic test

The catalytic activity of the Pd-STO was first tested on the oxidation of 1-phenylethanol (1-PE) to acetophenone (AP) (Table 1). The best catalytic performance was shown by Pd-STO(12.5) with an AP yield of 63% and a turnover number (TON = AP/Pd) of 172 (entry 2). Pd-STO (5.0) and Pd-STO(25.0) only demonstrated AP yields of 31% and 54%, respectively. The presence of mesoporous or the higher surface area of Pd-STO(12.5) is likely responsible for this higher performance; even the particle size of the perovskite is much larger than that of the others (Fig. 2). Thus, further experiments were studied using the Pd-STO(12.5) catalyst. STO itself did not show any catalytic activity under such conditions. Pd-STO(12.5) as-prepared at a higher temperature (433 K) exhibited an AP yield of only 36% due to the higher degree of crystallization (*i.e.*, drop in the surface area or porosity) (entry 4).

The as-prepared Pd-STO(12.5) catalyst demonstrated a maximum AP yield of only 63% (Table 2, entry 1). Interestingly, > 99% of the yield (TON up to 1070) could be obtained by the addition of molecular sieves (MS3A) into the reaction system (entry 2 and 3). MS3A itself did not show any catalytic activity under such conditions. We found that MS3A after reaction contained more water than that of the blank experiment (Fig. S6). This phenomenon is likely related to its ability to absorb the water byproduct, thus inhibited the water absorption on the perovskite catalyst surfaces (*i.e.*, deactivation) (Fig. S8). In the absence of MS3A, a small addition of water (0.03 g, 1.67 mmol) also decreased the AP yield by 11%. Besson et al. [15] reported that the presence of

Table 2
Effect of the catalyst pretreatments.

Entry	Pd-STO(12.5)	Conv./%	Yield/%	TON
1	As-prepared	63	63	172
2 ^a	As-prepared	> 99	> 99	273
3 ^b	As-prepared	98	98	1070
4 ^c	As-prepared	79	79	216
5 ^d	As-prepared	75	75	205
6 ^e	As-prepared	54	54	147
7	Calcined	37	37	101
8	Reduced	89	85	232

Reaction conditions: 1-PE/Pd = 273; 1-PE, 25 mg; Pd-STO(12.5), 12.5 mg; *n*-hexane, 2 mL; O₂, 0.1 MPa (balloon); 342 K; 24 h. Addition of:

^a MS3A, 100 mg.

^b MS3A, 100 mg; 1-PE/Pd = 1,092.

^c MS3A, 50 mg.

^d MS3A, 100 mg; water, 0.25 mL.

^e K₂CO₃, 100 mg.

water can promote the formation of geminal diol (by the hydration of aldehyde) which is subsequently dehydrogenated to acidic products. Instead, Steinhoff et al. [16] reported that the MS3A did not alter the influence of water but serves as a Brønsted base (Pd(OAc)₂/pyridine catalyst). In fact, the addition of external water inhibited the reaction significantly (entry 5). Moreover, the addition of the base K₂CO₃ (without MS3A) did not enhance the reaction at all (entry 6).

As expected, the calcined Pd-STO catalyst (923 K, 6 h, air) showed lower performance (Table 2, entry 7) due to a higher degree of crystallization, similar to the catalyst prepared at a higher hydrothermal temperature. Conversely, the reduction of the catalyst (573 K, 1 h, H₂) enhanced the reaction significantly (entry 8). The use of ethylene glycol (as a reducing agent) in the hydrothermal process also increased the catalytic activity (not shown). This result is consistent with the previous reports that suggested that Pd⁰ is the active phase [17,18]. However, a small amount of degradation products (*e.g.*, decarbonylation) may be produced due to the considerable initial activity of the pre-reduced catalyst [17]. The reduction process at high temperature could also promote the sintering of Pd⁰, thus, it is more difficult to reincorporate (lessen the recyclability). For the as-prepared catalyst, smaller particles of Pd⁰ could be generated by the *in situ* reduction of the substrate alcohols [18].

3.2.1. Solvent screening, reaction temperature and atmosphere

The use of an appropriate solvent was crucial for obtaining high catalytic performance (Table 3). Under such conditions, the highest AP yield (> 99%) was obtained by using *n*-hexane as the solvent (entry 1). Other non-polar solvents such as *n*-heptane, cyclohexane and toluene (entries 2–6) also exhibited higher AP yields than that of the polar solvents (entries 7–12). The use of non-polar solvents ensures no competition between the solvent and the substrate to adsorb onto the catalyst surfaces. Additionally, leaching of the active phase, as usually observed in highly polar solvents, can be minimized. A reaction at the reflux temperature of *n*-hexane (342 K) was optimum for O₂ to diffuse into the solution and thus be available for reaction. Notably, a complete conversion was also obtained of the reaction at the reflux temperatures of *n*-heptane and cyclohexane (entry 3 and 5, respectively). The complete conversion at 342 K was an exceptionally lower reaction temperature compared with that of the previous work with an AP yield of only 12% under such conditions (solvent: toluene) [10].

The Pd-STO perovskite showed catalytic activity even at temperatures as low as 298 K (Table 4, entry 1). The activity was increased by raising the reaction temperature and reached an optimum value at reflux conditions of 342 K (entry 4). At 323 K, we observed that the reduced catalyst also showed higher activity than the as-prepared catalyst

Table 3
Solvent screening.

Entry	Solvent	Conv./%	Yield/%
1	<i>n</i> -Hexane	> 99	> 99
2	<i>n</i> -Heptane	44	44
3 ^a	<i>n</i> -Heptane	> 99	> 99
4	Cyclohexane	67	67
5 ^b	Cyclohexane	> 99	> 99
6	Toluene	46	46
7	Trifluorotoluene	16	16
8	Acetonitrile	15	15
9	2-Propanol	36	36
10	Ethanol	26	26
11	DMF	31	31
12	1,4-Dioxane	35	35

Reaction conditions: 1-PE/Pd = 273; 1-PE, 25 mg; Pd-STO (12.5), 12.5 mg; solvent, 2 mL; O₂, 0.1 MPa (balloon); 342 K (*n*-hexane, refluxed); 24 h; MS3A, 100 mg.

^a Refluxed at 371 K.

^b Refluxed at 353 K.

Table 4
Effect of the reaction temperature and atmosphere.

Entry	Temp./K	Conv./%	Yield/%
1	298	19	19
2	323	22	22
3	333	56	56
4 ^a	342 (refluxed)	62(9)	62(9)
5 ^b	383 (refluxed)	49	49
6 ^c	323	36	36

Reaction conditions: 1-PE/Pd = 273; 1-PE, 25 mg; Pd-STO(12.5), 12.5 mg; *n*-hexane, 2 mL; O₂, 0.1 MPa (balloon); 4 h; MS3A, 100 mg.

^a The value in the parenthesis is of reaction under N₂.

^b Solvent, toluene.

^c Reduced Pd-STO(12.5).

(entry 6). Note that reaction under air (342 K, 24 h) demonstrated an AP yield of only 82% compared with the > 99% for a reaction under O₂. The reaction did not proceed smoothly under N₂ (entry 4, in the parenthesis), which suggests the critical role of O₂. A reaction at a much higher temperature (383 K, toluene as solvent) also still exhibited a high AP yield (entry 5), confirming the stability of the perovskite catalyst.

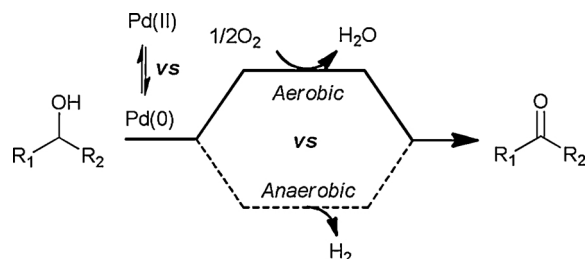
Since a small conversion still be observed under N₂ (Table 4, entry 4 (parenthesis)), we presume that O₂ probably originated from the perovskite. A gas consumption test revealed that O₂ was consumed almost stoichiometrically to the substrate at ca. 1:2 (Scheme 1). However, for reactions under N₂, the gas volume did not significantly change (it should be increased, if oxidant-free dehydrogenation occurs). Some researchers reported that Pd has an oxidant-free dehydrogenation ability. Unfortunately, under anaerobic conditions, the adsorbed hydrogen (or degradation products) was ineffectively removed from the catalyst surface [17].

3.2.2. Time profile and hot filtration test

The time profile for the oxidation reaction over Pd-STO(12.5) is shown in Fig. 5. An induction period was observed during the first hour of the reaction time. This period is likely related to the reduction process by the substrate alcohol to generate the active phase Pd⁰. Afterwards, the reaction progressed in time and reached completion after 24 h. No further reaction was observed after hot filtration (no leaching of the Pd species) that proved unequivocally that the reaction proceeded via heterogeneous catalysis. An ICP analysis of the filtrate after hot filtration did not indicate Pd leaching. Additionally, the Pd content of the reused catalyst remains the same (Table S2). In the absence of molecular sieves (MS3A), the reaction rate was slightly lower especially after a 3-h reaction time.

3.2.3. Substrate scopes

Various secondary alcohols have been tested as a substrate (Table 5). Mostly, aromatic secondary alcohols such as 1-phenylethanol (entry 1) and benzoin (entry 3) were easily oxidized compared with the others. In all cases, the selectivity to the corresponding products is



Scheme 1. Aerobic and oxidant-free (anaerobic) dehydrogenation of alcohols over the Pd-based catalyst.

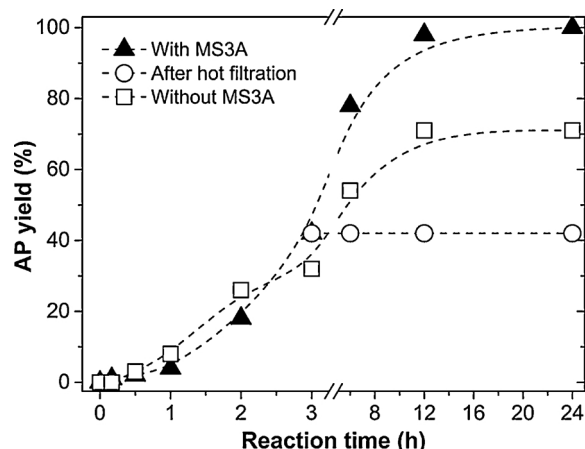


Fig. 5. Time profiles for the aerobic oxidation of 1-PE over Pd-STO(12.5) catalyst. Reaction conditions: 1-PE/Pd = 273, 1-PE, 25 mg; Pd-STO(12.5), 12.5 mg; *n*-hexane, 2 mL; O₂, 0.1 MPa (balloon); 342 K (refluxed); and MS3A, 100 mg.

Table 5
Substrate scopes for the secondary alcohols.

Entry	Substrate	Product	Conv./%	Yield/%
1			> 99	> 99
2			42	42
3			> 99	> 99
4			80	80
5			22	22
6			11	11
7			56	56
8			34	34

Reaction conditions: Substrate/Pd = 273; Pd-STO(12.5), 12.5 mg; *n*-hexane, 2 mL; O₂, 0.1 MPa (balloon); 342 K (refluxed); 24 h; MS3A, 100 mg.

almost 100%. We suggested that stability of the carbocation intermediate is highly pivotal for obtaining the high yield. An aromatic ring has ability to stabilize the adjacent carbocation over the resonance effect; thus the β -hydride elimination step is much easier. In contrast, the substrates with alicyclic substituents such as cyclopropyl (entry 2) and cyclohexyl (entry 4) were not smoothly converted. Lower conversions were also observed for other secondary aliphatic/cyclic alcohols (entry 5–8).

Due to the lower carbocation stability, primary alcohols were harder to oxidize (Table 6). The presence of an aromatic ring in benzyl alcohol (entry 1) leads to a higher yield, as mentioned above. The reduction treatment and the addition of a hydrogen acceptor such as cyclohexene (entries 2 and 3, respectively) could enhance the reactions. The complete conversion to benzaldehyde (entry 4) was obtained by the addition of K₂CO₃. By using TBHP as an oxidant, benzyl alcohol was exclusively oxidized to benzoic acid (entry 6). Neither the reduced catalyst nor the addition of a base could enhance the oxidation of the primary aliphatic alcohols (entries 7–9). In addition to carbocation stability, the primary aldehyde products may poison the catalyst by

Table 6
Substrate scopes for the primary alcohols.

Entry	Substrate	Product	Conv./%	Yield/%
1			38	38
2 ^a			64	64
3 ^b			55	55
4 ^c			> 99	> 99
5 ^d			0	0
6 ^e			> 99	0
7			7	7
8 ^a			7	7
9 ^c			7	7

Reaction conditions: Substrate/Pd = 273; Pd-STO(12.5), 12.5 mg; *n*-hexane, 2 mL; O₂, 0.1 MPa (balloon); 342 K (refluxed); 24 h; MS3A, 100 mg.

^a Reduced Pd-STO(12.5).

^b Addition of cyclohexene, 1 mol eq. to the substrate.

^c Addition of K₂CO₃, 55 mg.

^d Cat: K₂CO₃, 55 mg.

^e Addition of TBHP (70% in water), 0.5 mL.

strongly adsorbing on the metal surfaces [19].

3.2.4. Recyclability test

The Pd-STO catalyst could be easily separated from the reaction mixture by centrifugation. After being rinsed with *n*-hexane and dried under vacuum (at room temperature), the next reaction cycle was performed, as described above. The Pd-STO(12.5) catalyst could be recycled at least 4 times without significant loss of activity (Fig. 6). The impregnated catalyst (*imp*-Pd/STO) showed poor recyclability which is likely due to sintering (or leaching) of the active species (see: Fig. 4). Therefore, the incorporation of Pd into the perovskite was critical to maintaining its performance.

The perovskite phase remained unchanged, even after the third run (Fig. 7). In fact, perovskite is well known for its durability, especially at high temperature, which is thus more applicable for industry [4]. The high recyclability of the catalyst is likely due to the incorporation of Pd into the perovskite, which prevents leaching or Pd aggregation (which is commonly observed for supported Pd on conventional supports). This reversible process occurs easily because small Pd particles could be reduced or oxidized even at room temperature [14,18].

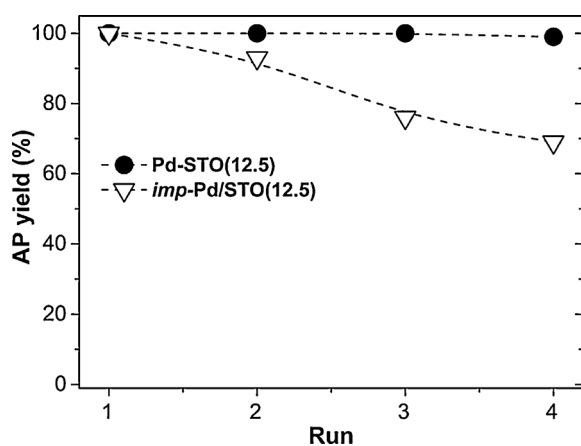


Fig. 6. Recyclability tests for Pd-STO(12.5) and *imp*-Pd/STO(12.5). Reaction conditions: 1-PE/Pd = 273; 1-PE, 25 mg; catalyst, 12.5 mg; *n*-hexane, 2 mL; O₂, 0.1 MPa (balloon); 342 K (refluxed); 24 h; and MS3A, 100 mg.

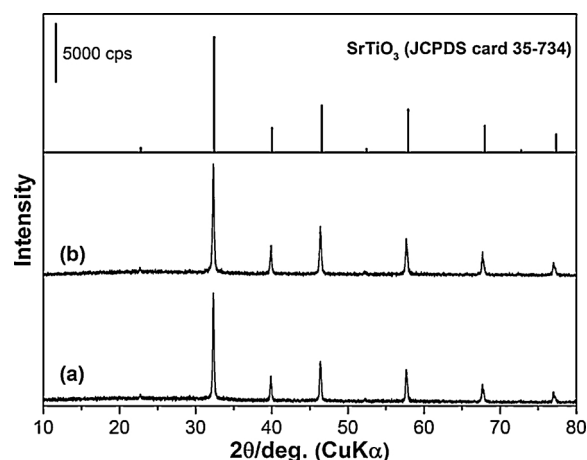


Fig. 7. Powder XRD patterns of Pd-STO(12.5): (a) fresh and (b) after the third run of the catalytic tests.

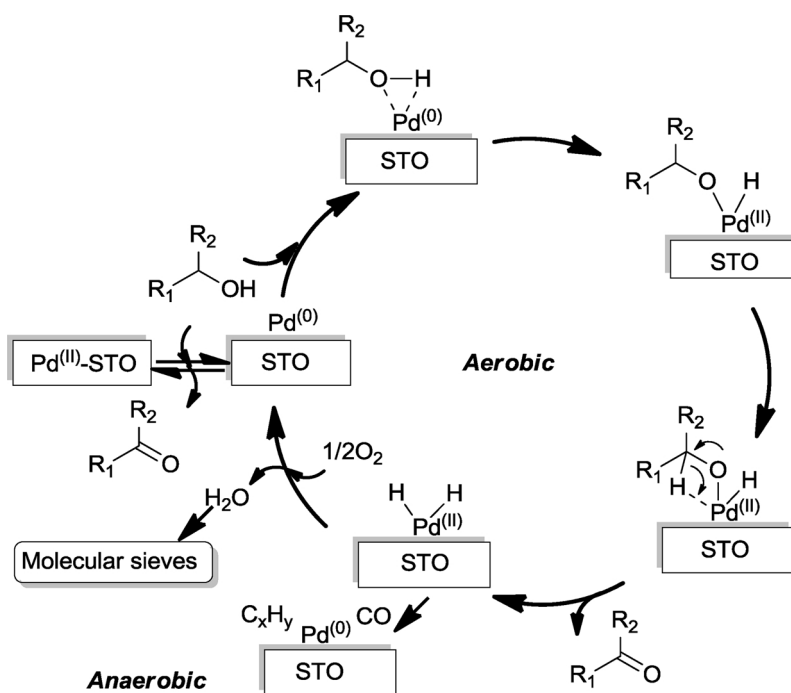
3.2.5. Plausible mechanism

Based on the results and discussion above, we proposed a plausible mechanism as shown in Scheme 2. The incorporated Pd is first reduced by the alcohols and then moved onto the perovskite face. This process produced aldehydes/ketones (Scheme S1); thus, under an oxygen-free condition, a small amount of product could be detected (Table 4, entry 4). Meanwhile, Pd could promote oxidant-free dehydrogenation; however, the adsorbed byproducts could not be effectively removed in the absence of oxygen [17]. This phenomenon was also observed by Kereszegi et al. [20] with 10.7% of conversion (Ar, Pd/Al₂O₃) and by Savara et al. [21] (N₂, Pd/C). Grunwaldt et al. [17] proved by using *in situ* XAS (X-ray absorption spectroscopy) that “Pd⁰ is the active phase for aerobic dehydrogenation”. Interestingly, after being reoxidized by O₂, the Pd⁰ on the surface could be reversibly reincorporated into the perovskite lattice, which will thus prevent leaching or sintering [6]. The lack of a significant inhibition effect of a radical scavenger (TEMPO, 1 mol eq. to Pd) suggests that the reaction did not proceed via a radical mechanism. Bürgi et al. [22] reported the formation of a Pd-alkoxide intermediate by *in situ* ATR spectroscopy analysis.

Hydrogen abstraction from the alcohol will produce adsorbed hydrogen while the oxidation state of Pd was increased. The adsorbed hydrogen could also be used for alkenes hydrogenation. We proved that aerobic dehydrogenation occurs by gas consumption testing as discussed above. The use of O₂ as an oxidant is highly desirable in green chemistry [23]. Some researchers proposed that the adsorbed hydrogen could be oxidized by O₂ to produce water. Oxygen could also remove the adsorbed decomposition byproducts, *i.e.*, CO [17]. A considerable increase in the reaction by the addition of molecular sieves suggests its role to absorb the water byproduct. Finally, Pd could be reversibly reincorporated into the lattice, thus maintaining its high recyclability.

4. Conclusion

Pd-STO perovskites with a tunable particle size and porosity have been successfully synthesized via low-temperature hydrothermal method (373 K) without any posterior calcination. Porosity of the Pd-STO perovskites play an important role for obtaining the high yield on alcohol oxidation with molecular oxygen. Both refluxing of the non-polar solvents and addition of molecular sieves enhanced the reaction yield significantly. We demonstrated that the recyclability could be maintained by the incorporation of Pd into the perovskites. We believe this facile method could also be applied for the fabrication of other transition metal-contained perovskite catalysts.



Scheme 2. A simplified mechanism for alcohol oxidation over the Pd-perovskite catalyst.

Acknowledgements

This study was financially supported in part by JSPS KAKENHI Grant Number 15K06565 and the JSPS Bilateral Joint Research Project (2014-2017).

Appendix A. Supplementary data

Supplementary data associated with this article can be found, in the online version, at <http://dx.doi.org/10.1016/j.mcat.2018.04.023>.

References

- [1] T. Screen, *Platin. Met. Rev.* 51 (2007) 87.
- [2] (a) N. Kakiuchi, T. Nishimura, M. Inoue, S. Uemura, *Bull. Chem. Soc. Jpn.* 74 (2001) 165; (b) G. Wu, G.L. Brett, E. Cao, A. Constantinou, P. Ellis, S. Kuhn, G.J. Hutchings, D. Bethell, A. Gavriilidis, *Catal. Sci. Technol.* 6 (2016) 4749; (c) F. Fotouhi-Far, H. Bashiri, M. Hamadani, *Propellants Explos. Pyrotech.* 42 (2017) 213.
- [3] (a) H. Tanaka, M. Uenishi, M. Taniguchi, I. Tan, K. Narita, M. Kimura, K. Kaneko, Y. Nishihata, J. Mizuki, *Catal. Today* 117 (321) (2006); (b) H. Tanaka, I. Tan, M. Uenishi, M. Taniguchi, M. Kimura, Y. Nishihata, J. Mizuki, *J. Alloys Compd.* 408–412 (2006) 1071.
- [4] (a) J. Zhu, H. Li, L. Zhong, P. Xiao, X. Xu, X. Yang, Z. Zhao, J. Li, *ACS Catal.* 4 (2014) 2917; (b) A. Mishra, R. Prasad, *Catal. Rev. Sci. Eng.* 56 (2014) 57; (c) S. Royer, D. Duprez, F. Can, X. Courtois, C. Batiot-Dupeyrat, S. Laassiri, H. Alamdari, *Chem. Rev.* 114 (2014) 10292; (d) H. Zhu, P. Zhang, S. Dai, *ACS Catal.* 5 (2015) 6370.
- [5] (a) C.H. Kim, G. Qi, K. Dahlberg, W. Li, *Science* 327 (2010) 1624; (b) V. Albaladejo-Fuentes, F.E. López-Suárez, M.S. Sánchez-Adsuar, M.J. Illán-Gómez, *Appl. Catal. A* 488 (2014) 189; (c) J.T. Mefford, W.G. Hardin, S. Dai, K.P. Johnston, K.J. Stevenson, *Nature Mater.* 13 (2014) 726; (d) S.K. Megarajan, S. Rayalu, M. Nishibori, Y. Teraoka, N. Labhsetwar, *ACS Catal.* 5 (2015) 301; (e) A. Staykov, H. Téllez, T. Akbay, J. Druce, T. Ishihara, J. Kilner, *Chem. Mater.* 27 (2015) 8273.
- [6] (a) Y. Nishihata, J. Mizuki, T. Akao, H. Tanaka, M. Uenishi, M. Kimura, T. Okamoto, N. Hamada, *Nature* 418 (2002) 164; (b) A. Eyssler, P. Mandaliev, A. Winkler, P. Hug, O. Safonova, R. Figi, A. Weidenkaff, D. Ferri, *J. Phys. Chem. C* 114 (2010) 4584; (c) I. Hamada, A. Uozumi, Y. Morikawa, A. Yanase, H. Katayama-Yoshida, *J. Am. Chem. Soc.* 133 (2011) 18506; (d) M.B. Katz, G.W. Graham, Y. Duan, H. Liu, C. Adamo, D.G. Schlom, X. Pan, *J. Am. Chem. Soc.* 133 (2011) 18090; (e) A. Essoumhi, S.E. Kazzouli, M. Bousmina, *J. Nanosci. Nanotechnol.* 14 (2014) 2012.
- [7] (a) U.G. Singh, J. Li, J.W. Bennett, A.M. Rappe, R. Seshadri, S.L. Scott, *J. Catal.* 249 (2007) 349; (b) K. Shiro, I. Yamada, N. Ikeda, K. Ohgushi, M. Mizumaki, R. Takahashi, N. Nishiyama, T. Inoue, T. Irifune, *Inorg. Chem.* 52 (2013) 1604; (c) M. Kimura, Y. Niwa, K. Uemura, T. Nagai, Y. Inada, M. Nomura, *Mater. Trans.* 54 (2013) 246.
- [8] (a) K. Zhou, H. Chen, Q. Tian, Z. Hao, D. Shen, X. Xu, *J. Mol. Catal. A Chem.* 189 (2002) 225; (b) S. Petrović, L. Karanović, P.K. Stefanov, M. Zdujić, A. Terlecki-Baričević, *Appl. Catal. B Environ.* 58 (2005) 133; (c) G.C.M. Rodríguez, K. Kelm, B. Saruhan, *Appl. Catal. A Gen.* 387 (2010) 173; (d) B. Kucharczyk, *Catal. Lett.* 145 (2015) 1237.
- [9] (a) E. Tzimpilis, N. Moschoudis, M. Stoukides, P. Bekiaroglou, *Appl. Catal. B Environ.* 84 (2008) 607; (b) E. Tzimpilis, N. Moschoudis, M. Stoukides, P. Bekiaroglou, *Appl. Catal. B Environ.* 87 (2009) 9; (c) R. Watanabe, Y. Sekine, H. Takamatsu, Y. Sakamoto, S. Aramaki, M. Matsukata, E. Kikuchi, *Top. Catal.* 53 (2010) 621; (d) X. Zhang, H. Li, Y. Li, W. Shen, *Catal. Lett.* 142 (2012) 118; (e) Z. Say, M. Dogac, E.I. Vovk, Y.E. Kalay, C.H. Kim, W. Li, E. Ozensoy, *Appl. Catal. B Environ.* 154–155 (2014) 51; (f) D.Y. Yoon, Y.J. Kim, J.H. Lim, B.K. Cho, S.B. Hong, I.S. Nam, J.W. Choung, *J. Catal.* 330 (2015) 71; (g) V.Y. Zenou, D.E. Fowler, R. Gautier, S.A. Barnett, K.R. Poepfelmeier, L.D. Marks, *Solid State Ionics* 296 (2016) 90.
- [10] I.B. Adilina, T. Hara, N. Ichikuni, N. Kumada, S. Shimazu, *Bull. Chem. Soc. Jpn.* 86 (2013) 146.
- [11] (a) S.K. Nikam, A.A. Athawale, *Mater. Chem. Phys.* 155 (2015) 104; (b) D.D. Athayde, D.F. Souza, A.M.A. Silva, D. Vasconcelos, E.H.M. Nunes, J.C. Diniz da Costa, W.L. Vasconcelos, *Ceram. Int.* 42 (2016) 6555.
- [12] E. Grabowska, *Appl. Catal. B Environ.* 186 (2016) 97.
- [13] (a) T. Sugimoto, T. Kojima, *J. Phys. Chem. C* 112 (2008) 18437; (b) T. Kojima, T. Sugimoto, *J. Phys. Chem. C* 112 (2008) 18445; (c) T. Sugimoto, T. Kojima, *J. Phys. Chem. C* 112 (2008) 18760; (d) T. Kojima, T. Baba, K. Ota, C. Yukita, K. Inamoto, N. Uekawa, *J. Ceram. Soc. Jpn.* 124 (2016) 1226.
- [14] A. Baylet, P. Marécot, D. Duprez, P. Castellazzi, G. Groppi, P. Forzatti, *Phys. Chem. Chem. Phys.* 13 (2011) 4607.
- [15] M. Besson, P. Gallezot, C. Pinel, *Chem. Rev.* 114 (2014) 1827.
- [16] B.A. Steinhoff, A.E. King, S.S. Stahl, *J. Org. Chem.* 71 (2006) 1861.
- [17] (a) J. Grunwaldt, C. Keresszegi, T. Malat, A. Baiker, *J. Catal.* 213 (2003) 291; (b) J. Grunwaldt, M. Caravati, A. Baiker, *J. Phys. Chem. B* 110 (2006) 25586.
- [18] A. Jürgensen, N. Heutz, H. Raschke, K. Merz, R. Hegenröder, *Anal. Chem.* 87 (2015) 7848.
- [19] J. Yi, J.T. Miller, D.Y. Zemlyanov, R. Zhang, P.J. Dietrich, F.H. Ribeiro, S. Suslov, M.M. Abu-Omar, *Angew. Chem.* 126 (2014) 852.
- [20] C. Keresszegi, T. Bürgi, T. Mallat, A. Baiker, *J. Catal.* 211 (2002) 244.
- [21] (a) A. Savara, C.E. Chan-Thaw, I. Rossetti, A. Villa, L. Prati, *ChemCatChem* 6 (2014) 3464; (b) A. Savara, I. Rossetti, C.E. Chan-Thaw, L. Prati, A. Villa, *ChemCatChem* 8 (2016) 2482.
- [22] (a) T. Bürgi, M. Bieri, *J. Phys. Chem. B* 108 (2004) 13364; (b) T. Bürgi, *J. Catal.* 229 (2005) 55.
- [23] (a) T. Matsumoto, M. Ueno, N. Wang, S. Kobayashi, *Chem. Asian J.* 3 (2008) 196; (b) C. Parmeggiani, F. Cardona, *Green Chem.* 14 (2012) 547.